Beam Allocation based on Deep Learning for Wideband mmWave Massive MIMO

Pengju Zhang, Chenhao Qi
School of Information Science and Engineering, Southeast University, Nanjing, China
Email: {zpj, qch}@seu.edu.cn

ICC 2022 - IEEE International Conference on Communications | 978-1-5386-8347-7/22/$31.00 ©2022 IEEE | DOI: 10.1109/ICC45855.2022.9838974

***Abstract*—Beam allocation is considered for wideband multiuser mmWave massive MIMO systems. By introducing the interference-free achievable rate, the analog precoder and the digital precoder is decoupled for the beam allocation problem. Then the beam allocation is treated as a multi-label classification problem and a deep learning-based beam allocation (DLBA) scheme is proposed, where a convolutional neural network is trained offline using the simulated environments to predict the beam allocation for all the users. In order to avoid the beam conflict and maximize the sum-rate, a rule to avoid the beam conflict is also proposed. Simulation results demonstrate that the DLBA scheme can substantially reduce the computational complexity with a marginal sacrifice of sum-rate performance, compared to the existing schemes.**

***Index Terms*—Beam allocation, deep learning, massive MIMO, mmWave communications**

I. Introduction

Due to large bandwidth of millimeter wave (mmWave) communications and high spectral efficiency of massive MIMO, mmWave massive MIMO is considered as one of the most promising key technologies for next-generation wireless communications [1], [2]. Early work focuses on narrowband mmWave massive MIMO channels, but the experimental results show that the mmWave massive MIMO channels are wideband. Compared to the narrowband channels, the wideband channels are frequency-selective [3]. To deal with the frequency-selective fading, orthogonal frequency division multiplexing (OFDM) is typically adopted by mmWave massive MIMO [4].

To reduce the hardware complexity, we employ hybrid precoding including analog precoding and digital precoding for wideband mmWave MIMO OFDM systems [5]. In [6], by exploiting the sparse structure of mmWave MIMO channel and formulating the hybrid precoding design problem as a sparse reconstruction one, the authors propose a spatially sparse precoding algorithm based on simultaneous orthogonal matching pursuit (SOMP). In [7], aiming at maximizing the sum-rate of multiple users, a two-stage (TS) limited feedback multiuser hybrid precoding scheme is proposed. However, neither [6] nor [7] considers the beam conflict, which occurs if multiple spatially-close users employ the same analog beam. Note that beam conflict causes the low rank of the analog precoder matrix and results in the severe multiuser interference that cannot be mitigated by the digital precoder. In [8], the design of analog precoder is transformed into an assignment problem aiming at selecting mutually different codewords from the codebook for different users to achieve the maximum sum-rate, where a Hungarian-based codeword assignment scheme is proposed.

In this paper, we consider the beam allocation problem for wideband multiuser mmWave massive MIMO systems. By introducing the interference-free (IF) achievable rate, we decouple the analog precoder and the digital precoder. Then we treat the beam allocation as a multi-label classification problem and a deep learning-based beam allocation (DLBA) scheme is proposed, where a convolutional neural network (CNN) is trained offline using the simulated environments to predict the beam allocation for all the users online. In order to avoid the beam conflict and maximize the sum-rate, we propose a rule to avoid the beam conflict.

Notations: Symbols for vectors (lower case) and matrices (upper case) are in boldface. For a vector $\boldsymbol{a}$, $[\boldsymbol{a}]_m$ and $\|\boldsymbol{a}\|_2$ denotes its mth entry and l_2-norm. For a three-dimensional matrix $\boldsymbol{A}$, $\boldsymbol{A}^{(i)}$ denotes the ith two-dimensional matrix. For a two-dimensional matrix $\boldsymbol{A}$, $[\boldsymbol{A}]_{m,:}$, $[\boldsymbol{A}]_{:,n}$, $[\boldsymbol{A}]_{m,n}$, $\boldsymbol{A}^{\mathrm{T}}$, $\boldsymbol{A}^{-1}$, $\boldsymbol{A}^{\mathrm{H}}$ and $\|\boldsymbol{A}\|_{\mathrm{F}}^2$ denote the mth row, the nth column, the entry on the mth row and nth column, the transpose, the inverse, the conjugate transpose (Hermitian), and Frobenius norm, respectively. $\boldsymbol{I}_K$ denotes an $K \times K$ identity matrix. $\mathbb{E}\{\cdot\}$ and $\mathcal{CN}(0, \sigma^2)$ denote the expectation and the complex Gaussian distribution with the zero mean and the variance being σ^2, respectively. The symbols $\mathbb{C}$ and $\mathbb{R}$ denote the set of complex-valued numbers and the set of real-valued numbers, respectively.

II. Problem Formulation

We consider a wideband multiuser mmWave massive MIMO system, whose block diagram is shown in Fig. 1. To deal with the frequency-selective fading of the wideband mmWave channels, we typically adopt OFDM modulation. Suppose the number of OFDM subcarriers is U. The base station (BS) equipped with K RF chains and N_{BS} uniform linear array (ULA) antennas, transceives K independent data streams. According to the hybrid precoding structure of mmWave massive MIMO system, we assume $1 \leq K \ll N_{\mathrm{BS}}$. Each user is equipped with a single RF chain and a single antenna.

During the downlink transmission, the transmitted signal is denoted by

$$\boldsymbol{X} \triangleq [\boldsymbol{x}_1, \boldsymbol{x}_2, \ldots, \boldsymbol{x}_U] \in \mathbb{C}^{K \times U} \tag{1}$$

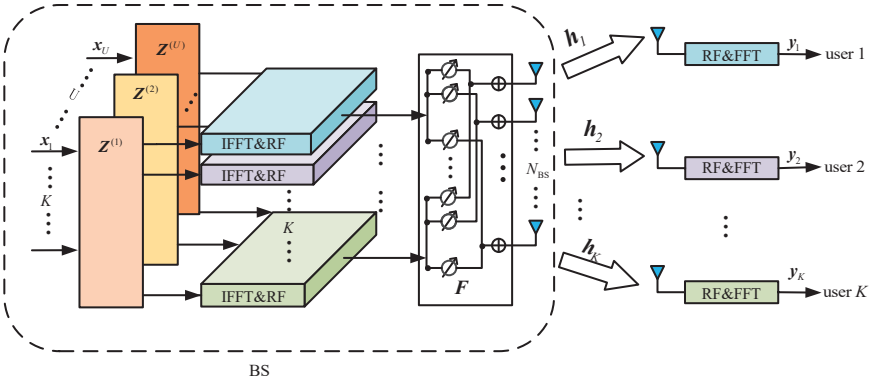

Fig. 1. Block diagram of wideband multiuser mmWave massive MIMO system.

where $[\boldsymbol{X}]_{k,u}$ represents the signal sent by the BS to the kth user on the uth OFDM subcarrier, for $k = 1, 2, \ldots, K$ and $u = 1, 2, \ldots, U$, and $\boldsymbol{x}_u \in \mathbb{C}^K$ is the transmit signal vector by the BS to all the K users on the uth OFDM subcarrier. The received signal by all the K users on all the U OFDM subcarriers form a matrix

$$\boldsymbol{Y} \triangleq [\boldsymbol{y}_1^{\mathrm{T}}, \boldsymbol{y}_2^{\mathrm{T}}, \ldots, \boldsymbol{y}_K^{\mathrm{T}}]^{\mathrm{T}} \in \mathbb{C}^{K \times U} \tag{2}$$

where $[\boldsymbol{Y}]_{k,u}$ represents the signal received by the kth user on the uth OFDM subcarrier, and $\boldsymbol{y}_k \in \mathbb{C}^U$ is the received signal vector by the kth users on all the OFDM subcarriers.

For the uth OFDM subcarrier, $u = 1, 2, \ldots, U$, we have

$$[\boldsymbol{Y}]_{:,u} = \boldsymbol{H}^{(u)} \boldsymbol{F} \boldsymbol{Z}^{(u)} \boldsymbol{x}_u + [\boldsymbol{\Phi}]_{:,u} \tag{3}$$

where $\boldsymbol{H}^{(u)} \in \mathbb{C}^{K \times N_{\mathrm{BS}}}$ is the frequency-domain downlink channel matrix on the uth OFDM subcarrier,

$$\boldsymbol{Z}^{(u)} \triangleq \left[\boldsymbol{z}_1^{(u)}, \boldsymbol{z}_2^{(u)}, \ldots, \boldsymbol{z}_K^{(u)}\right] \in \mathbb{C}^{K \times K} \tag{4}$$

is the digital precoder for the uth OFDM subcarrier,

$$\boldsymbol{F} \triangleq [\boldsymbol{f}_1, \boldsymbol{f}_2, \ldots, \boldsymbol{f}_K] \in \mathbb{C}^{N_{\mathrm{BS}} \times K} \tag{5}$$

is the analog precoder, and $[\boldsymbol{\Phi}]_{:,u} \in \mathbb{C}^K \sim \mathcal{CN}(\boldsymbol{0}, \sigma^2 \boldsymbol{I}_K)$ is the noise term obeying the complex Gaussian distribution with zero mean and variance of σ^2. Since the angle of departure (AoD) and angle of arrival (AoA) are the same for different OFDM subcarriers, the analog precoder $\boldsymbol{F}$ is the same for different OFDM subcarriers. Note that $\boldsymbol{F}$ is typically implemented by a phase-shifter network, where each entry of $\boldsymbol{F}$ has a constant modulus and only its phase can be changed.

To satisfy the constraint of maximum transmit power P_T, we have $\mathbb{E}\left\{\boldsymbol{x}_u \boldsymbol{x}_u^{\mathrm{H}}\right\} = \frac{P_T}{KU} \boldsymbol{I}_K$.

Moreover, we have

$$\left\|\boldsymbol{F} \boldsymbol{Z}^{(u)}\right\|_{\mathrm{F}}^2 = 1 \tag{6}$$

implying that the hybrid precoder does not provide any power gain.

The mmWave massive MIMO downlink channel vector between the BS and the kth user is assumed to be frequency-selective with a delay of d taps in the time domain, $d = 1, 2, \ldots, D$, and can be expressed as

$$\boldsymbol{c}_k(d) = \sqrt{\frac{N_{\mathrm{BS}}}{L_k}} \sum_{l=1}^{L_k} \alpha_{l,k} p(dT_s - \tau_{l,k}) \boldsymbol{a}^{\mathrm{H}}(N_{\mathrm{BS}}, \phi_{l,k}) \tag{7}$$

where L_k denotes the number of resolvable channel paths, $\alpha_{l,k}$ is the complex-valued channel gain, $\tau_{l,k}$ is the multipath delay, $\phi_{l,k} \in (-\frac{\pi}{2}, \frac{\pi}{2}]$ is the AoD of the lth path, $p(t)$ is the pulse-shaping function, T_s is the sampling interval and D is the number of maximum channel delay taps. The channel steering vector of the BS, denoted by $\boldsymbol{a}(N_{\mathrm{BS}}, \phi_{l,k}) \in \mathbb{C}^{N_{\mathrm{BS}}}$, can be expressed as

$$\boldsymbol{a}(N_{\mathrm{BS}}, \phi_{l,k}) \triangleq \frac{1}{\sqrt{N_{\mathrm{BS}}}} \left[1, e^{j\pi \sin \phi_{l,k}}, \ldots, e^{j(N_{\mathrm{BS}}-1)\pi \sin \phi_{l,k}}\right]^{\mathrm{T}} \tag{8}$$

where the antennas are placed with half wavelength interval.

In fact, $\boldsymbol{H}^{(u)}$ in (3) can be further expressed as

$$(\boldsymbol{H}^{(u)})^{\mathrm{T}} \triangleq \left[(\boldsymbol{h}_1^{(u)})^{\mathrm{T}}, (\boldsymbol{h}_2^{(u)})^{\mathrm{T}}, ..., (\boldsymbol{h}_K^{(u)})^{\mathrm{T}}\right] \tag{9}$$

where $\boldsymbol{h}_k^{(u)} \in \mathbb{C}^{1 \times N_{\mathrm{BS}}}$ is the frequency-domain channel vector between the BS and the kth user on the uth OFDM subcarrier. Given $\boldsymbol{c}_k(d)$ in (7), $\boldsymbol{h}_k^{(u)}$ can be expressed as

$$\boldsymbol{h}_k^{(u)} = \sum_{d=0}^{D-1} \boldsymbol{c}_k(d) e^{-j\frac{2\pi u}{U} d}, \ u = 1, 2, \ldots, U \tag{10}$$

which is essentially the U-point discrete Fourier transform (DFT) of $\boldsymbol{c}_k(d)$.

To fast generate the analog precoder, each column of $\boldsymbol{F}$ is selected from a predefined codebook $\boldsymbol{\mathcal{F}}$. We adopt the widely used DFT codebook as [9]

$$\boldsymbol{\mathcal{F}} \triangleq \{\boldsymbol{f}(n), n = 1, 2, \ldots, N_{\mathrm{BS}}\} \tag{11}$$

where the nth codeword in the codebook is

$$\boldsymbol{f}(n) \triangleq \boldsymbol{a}\left(N_{\mathrm{BS}}, -1 + \frac{(2n-1)}{N_{\mathrm{BS}}}\right) \tag{12}$$

Base on (3), the signal received by the kth user on the uth OFDM subcarrier can be expressed as

$$\begin{aligned}[\boldsymbol{Y}]_{k,u} &= \boldsymbol{h}_k^{(u)}\boldsymbol{F}\boldsymbol{Z}^{(u)}[\boldsymbol{x}]_u + [\boldsymbol{\Phi}]_{k,u} \\ &= \boldsymbol{h}_k^{(u)}\boldsymbol{F}\boldsymbol{z}_k^{(u)}[\boldsymbol{X}]_{k,u} \\ &\quad + \boldsymbol{h}_k^{(u)}\boldsymbol{F}\sum_{i=1,i\neq k}^{K}\boldsymbol{z}_i^{(u)}[\boldsymbol{X}]_{i,u} + [\boldsymbol{\Phi}]_{k,u}.\end{aligned} \tag{13}$$

We denote the achievable rate of the kth user on the uth OFDM subcarrier by $[\boldsymbol{R}]_{k,u}$, which can be expressed as

$$[\boldsymbol{R}]_{k,u} = \log_2\left(1 + \frac{\frac{P_T}{KU}\left|\boldsymbol{h}_k^{(u)}\boldsymbol{F}\boldsymbol{z}_k^{(u)}\right|^2}{\frac{P_T}{KU}\sum_{i\neq k}\left|\boldsymbol{h}_k^{(u)}\boldsymbol{F}\boldsymbol{z}_i^{(u)}\right|^2 + \sigma^2}\right). \tag{14}$$

It is seen that there exists the multiuser interference in the denominator of (14), which will degrade the performance of $[\boldsymbol{R}]_{k,u}$.

Therefore, the optimizing problem to maximize the sum-rate of all the K users on all the U OFDM subcarriers can be expressed as

$$\max_{\boldsymbol{F},\boldsymbol{Z}} \quad \frac{1}{U}\sum_{u=1}^{U}\sum_{k=1}^{K}[\boldsymbol{R}]_{k,u} \tag{15a}$$

$$\text{s.t.} \quad \boldsymbol{f}_k \in \boldsymbol{\mathcal{F}},\ k = 1,2,\ldots,K \tag{15b}$$

$$\boldsymbol{f}_v \neq \boldsymbol{f}_w,\ v,w = 1,2,\ldots,K, v\neq w \tag{15c}$$

$$(6). \tag{15d}$$

Note that (15b) indicates that the analog precoder is selected from the predefined codebook $\boldsymbol{\mathcal{F}}$ in (11). The constraint (15c) ensures that different codewords from $\boldsymbol{\mathcal{F}}$ are selected to serve different users, which can avoid the *beam conflict*. Once the *beam conflict* occurs, i.e., two or more users select the same codeword from $\boldsymbol{\mathcal{F}}$, $\boldsymbol{F}$ will be low-rank and the multiuser interference can not be mitigated by the digital precoder $\boldsymbol{Z}$, which substantially impairs the sum-rate performance.

The optimization problem (15) is challenging due to the difficulty of multiuser codeword selection and the coupling between $\boldsymbol{F}$ and $\boldsymbol{Z}$, hence the problem (15) is a typical non-convex multivariate mixed integer non-linear problem of which the optimum is difficult to find. Therefore, we adopt the hierarchical design idea to decouple $\boldsymbol{F}$ and $\boldsymbol{Z}$ and treat the beam allocation as a multi-label classification problem.

III. Improved DLBA Scheme Design

In practice, we typically first design the analog precoder to make the beams align with the mmWave MIMO channel, and then design the digital precoder to mitigate the interference among different user streams, indicating that we first design $\boldsymbol{F}$ and then design $\boldsymbol{Z}$. To obtain the optimal solution of $\boldsymbol{F}$, we need to find K best codewords from totally N_{BS} codewords in $\boldsymbol{\mathcal{F}}$. It requires to traverse $(N_{\mathrm{BS}})^K$ kinds of codeword combinations. For each kind of codeword combination, we need to design the corresponding digital precoder to compute the sum-rate. From all kinds of codeword combinations, we finally select the one with the largest sum-rate. However, the computational complexity is prohibitively high.

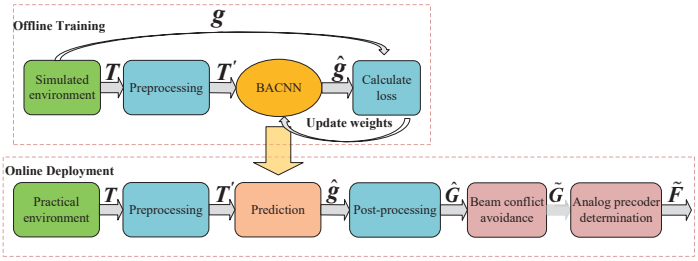

Fig. 2. Block diagram of the DLBA scheme.

Note that (15c) guarantees there is no beam conflict and therefore the multiuser interference is small. Then the function of $\boldsymbol{Z}$ to mitigate the multiuser interference can be temporarily neglected when designing $\boldsymbol{F}$. Once $\boldsymbol{F}$ is designed, we then design $\boldsymbol{Z}$, which can decouple $\boldsymbol{F}$ and $\boldsymbol{Z}$ and substantially reduce the computational complexity. To this end, we introduce the IF achievable rate of the kth user on the uth OFDM subcarrier by $[\boldsymbol{R}]_{k,u}^{\mathrm{IF}}$, which can be expressed as

$$[\boldsymbol{R}]_{k,u}^{\mathrm{IF}} = \log_2\left(1 + \frac{P_T\left|\boldsymbol{h}_k^{(u)}\boldsymbol{f}_k\right|^2}{KU\sigma^2}\right). \tag{16}$$

Then (15) can be converted into

$$\max_{\boldsymbol{F}} \quad \frac{1}{U}\sum_{u=1}^{U}\sum_{k=1}^{K}[\boldsymbol{R}]_{k,u}^{\mathrm{IF}} \tag{17a}$$

$$\text{s.t.} \quad \boldsymbol{f}_k \in \boldsymbol{\mathcal{F}},\ k = 1,2,\ldots,K \tag{17b}$$

$$\boldsymbol{f}_v \neq \boldsymbol{f}_w,\ v,w = 1,2,\ldots,K, v\neq w. \tag{17c}$$

It is a typical codeword selection problem, which can be solved by the Hungarian algorithm. To reduce the computational complexity of the Hungarian algorithm so that the codeword selection can be performed in real-time, we propose a DLBA scheme, which includes the offline training and online deployment stages. As shown in Fig. 2, during the offline training stage, we use the simulated environment to train the proposed convolutional neural network for beam allocation (BACNN). During the online deployment stage, we use the trained BACNN for codeword selection by predicting the beam allocation matrix. Then based on the beam conflict avoidance rule, we update the beam allocation matrix so that the constraint (17c) can be strictly satisfied. The final output is the designed analog precoder. The detailed steps of the DLBA scheme are summarized in **Algorithm 1**.

We perform the beam sweeping using all the codewords in $\boldsymbol{\mathcal{F}}$ for all the users [10]. Then we can compute the IF achievable rate of the kth user as

$$r(k,n) = \frac{1}{U}\sum_{u=1}^{U}\log_2\left(1 + \frac{P_T\left|\boldsymbol{h}_k^{(u)}\boldsymbol{f}(n)\right|^2}{KU\sigma^2}\right) \tag{18}$$

Algorithm 1 DL-based Codeword Selection and Analog Precoding

1: **Input:** $\boldsymbol{\mathcal{F}}, \boldsymbol{T}, \boldsymbol{g}, J, N_{\mathrm{BS}}, K$.
2: (*Preprocessing*)
3: For each row of $\boldsymbol{T}$, keep the largest J entries and set the other entries to be zero.
4: Obtain $\boldsymbol{T}^{'}$ based on $\boldsymbol{T}$ by deleting its all-zero columns and fixing its size.
5: (*Beam Allocation Training and Prediction*)
6: Input training data $\boldsymbol{T}^{'}$ and the label $\boldsymbol{g}$ to the BACNN for offline training.
7: Feed online data $\boldsymbol{T}^{'}$ to the trained BACNN, obtaining its output as $\widehat{\boldsymbol{g}}$.
8: (*Post-processing*)
9: Recover $\widehat{\boldsymbol{G}}'$ from $\widehat{\boldsymbol{g}}$ and recover $\widehat{\boldsymbol{G}}$ from $\widehat{\boldsymbol{G}}'$.
10: (*Beam conflict avoidance*)
11: Obtain $\widetilde{\boldsymbol{G}}$ by applying the rule to avoid beam conflict.
12: Determine $\widetilde{\boldsymbol{F}}$ based on $\widetilde{\boldsymbol{G}}$.
13: **Output:** $\widetilde{\boldsymbol{F}}$.

if the BS uses $\boldsymbol{f}(n)$ to serve the kth user, $k = 1, 2, \ldots, K$, $n = 1, 2, \ldots, N_{\mathrm{BS}}$. In fact, we may substitute $\boldsymbol{f}_k$ by $\boldsymbol{f}(n)$ in (16) and then make summation of $[\boldsymbol{R}]_{k,u}^{\mathrm{IF}}$ for all the OFDM subcarriers, i.e., $u = 1, 2, \ldots, U$, so that (18) can be figured out.

We define a complex-valued matrix $\boldsymbol{T} \in \mathbb{C}^{K \times N_{\mathrm{BS}}}$, with $[\boldsymbol{T}]_{k,n}$ expressed as

$$[\boldsymbol{T}]_{k,n} \triangleq \mathcal{J}\left(r(k,n), \gamma_k\right) \tag{19}$$

where $\mathcal{J}(x, y)$ is a threshold function as

$$\mathcal{J}(x,y) \triangleq \begin{cases} x, & \text{if } x \geq y, \\ 0, & \text{else.} \end{cases} \tag{20}$$

In (19), γ_k is a threshold to control the number of candidate codewords for the kth user. Given the number of candidate codewords for each user, denoted as J $(2 \leq J \leq N_{\mathrm{BS}})$, we may set γ_k as the the Jth largest value of $\{r(k,n),\ n = 1, 2, \ldots, N_{\mathrm{BS}}\}$. By using the candidate codewords, each user can have more choices when beam conflict occurs.

Next we define a binary matrix $\boldsymbol{G} \in \{0,1\}^{K \times N_{\mathrm{BS}}}$, which is introduced to store the results of beam allocation. If $\boldsymbol{f}(n)$ is selected to serve the kth user, then $[\boldsymbol{G}]_{k,n} = 1$; otherwise, $[\boldsymbol{G}]_{k,n} = 0$. Then (17) can be rewritten as

$$\max_{\boldsymbol{G}} \ \sum_{k=1}^{K} \sum_{n=1}^{N_{\mathrm{BS}}} [\boldsymbol{T}]_{k,n} [\boldsymbol{G}]_{k,n} \tag{21a}$$

$$\text{s.t.} \ \sum_{k=1}^{K} [\boldsymbol{G}]_{k,n} \leq 1, \ n = 1, 2, \ldots, N_{\mathrm{BS}} \tag{21b}$$

$$\sum_{n=1}^{N_{\mathrm{BS}}} [\boldsymbol{G}]_{k,n} = 1, \ k = 1, 2, \ldots, K \tag{21c}$$

where (21b) indicates that each codeword can be selected at most once and (21c) indicates that each user can select only one codeword.

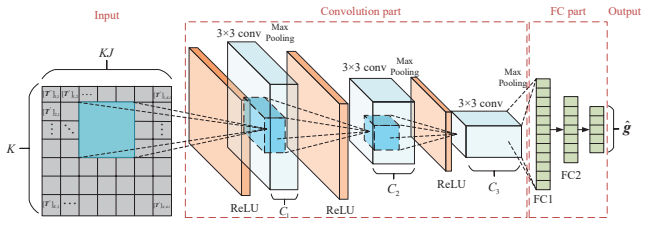

Fig. 3. BACNN model for DLBA scheme.

Each row of $\boldsymbol{G}$ is a one-hot vector, which is the output of the single-label classification problem. Then we concatenate each row of $\boldsymbol{G}$, obtaining a row vector $\boldsymbol{g} \in \mathbb{R}^{1 \times (K N_{\mathrm{BS}})}$ as training label, which can be treated as the output of a multi-label classification problem. On the other hand, $\boldsymbol{T}$ resembles an image with $K \times N_{\mathrm{BS}}$ pixels. Note that the CNN proves to be efficient to deal with the image classification problem. Therefore, it is natural to use the CNN to learn the features of $\boldsymbol{T}$ to solve this multi-label classification problem [11]. To this end, we propose a BACNN for beam allocation in mmWave massive MIMO system.

As shown in Fig. 3, the BACNN consists of convolution part and fully connected (FC) part. The convolution part is composed of three sub-blocks sequentially connected. Each sub-block consists of a rectified linear unit (ReLU) layer, a convolution layer and a max-pooling layer, where the ReLU layer can be represented as $f_{\mathrm{Re}}(x) = \max(0, x)$. The ReLU layers prevent negative values and therefore guarantee the non-linearity of the BACNN. The convolution layer performs two-dimensional spatial convolution for data. The convolution layers in three sub-blocks are set to be the same size 3×3 but different depth $C_1 = 16$, $C_2 = 32$ and $C_3 = 64$. The max-pooling layers, which are used to reduce data size and speed up the computation, are set to be the same size 2×2. In addition, the zero-padding is used to ensure that the size of input data matches the convolution kernel. FC part, which follows convolution part, consists of two FC layers with 512 and 256 neurons, respectively.

To reduce the storage overhead of $\boldsymbol{T}$, we need to make some preprocessing on $\boldsymbol{T}$. First, for each row of $\boldsymbol{T}$, we keep the largest J entries and set the other entries zero. Then we delete all-zero columns from $\boldsymbol{T}$, obtaining $\boldsymbol{T}^{'} \in \mathbb{R}^{K \times N^{'}}$, since the codewords corresponding to these columns are not candidates for any user. Note that we have $K \leq N' \leq N_{\mathrm{BS}}$. Since N' is variable, which brings challenge for the CNN, we need to find a upper bound for N' so that the size of input data to the CNN is fixed. In practice, N_{BS} is typically larger than 128, while J and K are around 4 and 16, respectively. In the context, we have $K \leq N' \leq KJ \leq N_{\mathrm{BS}}$, where KJ is a better upper bound for N' than N_{BS}, from the perspective of reducing the storage overhead of $\boldsymbol{T}'$. By adding $KJ - N^{'}$ zero columns on the right of $\boldsymbol{T}'$, we obtain a fixed size $\boldsymbol{T}' \in \mathbb{R}^{K \times (KJ)}$ and take $\boldsymbol{T}'$ as the input of the BACNN.

We denote the output of the BACNN as $\widehat{\boldsymbol{g}} \in \mathbb{R}^{1 \times (K^2 J)}$,

where $\widehat{\boldsymbol{g}}$ is a prediction of $\boldsymbol{g}$. Opposite to the procedures obtaining $\boldsymbol{g}$ from $\boldsymbol{G}$, we recover $\widehat{\boldsymbol{G}}' \in \mathbb{R}^{K\times(KJ)}$ from $\widehat{\boldsymbol{g}}$. Also opposite to the procedures obtaining $\boldsymbol{T}'$ from $\boldsymbol{T}$, we recover $\widehat{\boldsymbol{G}} \in \mathbb{R}^{K\times N_{\mathrm{BS}}}$ from $\widehat{\boldsymbol{G}}'$.

In order to satisfy (21c) to avoid the beam conflict and therefore maximize the sum-rate, we propose a rule as follows. For each row of $\widehat{\boldsymbol{G}}$, we set the largest entry to be one and the other entries to be zero, obtaining a binary matrix $\widetilde{\boldsymbol{G}}$, which ensures the constraint in (21b). If the summation of any column of $\widetilde{\boldsymbol{G}}$ is larger than one, there is beam conflict. If there exists an integer N, where the summation of the Nth column of $\widetilde{\boldsymbol{G}}$ is $M(M>1)$, M users denoted as k_1, k_2, …, k_M are involved in the beam conflict. We sort $\{[\widehat{\boldsymbol{G}}]_{k_m,N},\ m=1,2,\ldots,M\}$ in descending order as $[\widehat{\boldsymbol{G}}]_{\widehat{k}_1,N} \geq [\widehat{\boldsymbol{G}}]_{\widehat{k}_2,N} \geq \ldots \geq [\widehat{\boldsymbol{G}}]_{\widehat{k}_M,N}$.

1) The codeword $\boldsymbol{f}(N)$ is allocated to the $\widehat{k}_1$th user.
2) For the $\widehat{k}_2$th user, we denote the indices of his candidate codewords that have not yet been allocated to any users as $\boldsymbol{\Omega}$. We select the codeword with the index as

$$\widehat{i} = \arg\max_{i\in\boldsymbol{\Omega}} \ [\boldsymbol{T}]_{k_2,i} \tag{22}$$

for the $\widehat{k}_2$th user. Then we set

$$[\widetilde{\boldsymbol{G}}]_{\widehat{k}_2,N} = 0,\ [\widetilde{\boldsymbol{G}}]_{\widehat{k}_2,\widehat{i}} = 1. \tag{23}$$

3) We repeat 2) for the $\widehat{k}_3$th, …, $\widehat{k}_M$th user.

After applying the rule to avoid the beam conflict, the summation of any column of $\widetilde{\boldsymbol{G}}$ is no larger than one and the number of nonzero entries of $\widetilde{\boldsymbol{G}}$ is K. For each nonzero entry of $\widetilde{\boldsymbol{G}}$, the row index and the column index are denoted as k and $\widetilde{n}$, respectively. Then the codeword from $\boldsymbol{\mathcal{F}}$ allocated to the kth user is $\widetilde{\boldsymbol{f}}_k = \boldsymbol{f}(\widetilde{n})$, $k=1,2,\ldots,K$. Finally, the designed analog precoder is

$$\widetilde{\boldsymbol{F}} \triangleq \left[\widetilde{\boldsymbol{f}}_1, \widetilde{\boldsymbol{f}}_2, \ldots, \widetilde{\boldsymbol{f}}_K\right]. \tag{24}$$

After $\widetilde{\boldsymbol{F}}$ is determined, we define the equivalent channel matrix $\boldsymbol{H}_e^{(u)}$ as

$$\boldsymbol{H}_e^{(u)} \triangleq \boldsymbol{H}^{(u)}\widetilde{\boldsymbol{F}} \tag{25}$$

for $u=1,2,\ldots,U$. Based on (25), (3) can be rewritten as

$$[\boldsymbol{Y}]_{:,u} = \boldsymbol{H}_e^{(u)}\boldsymbol{Z}^{(u)}\boldsymbol{x}_u + [\boldsymbol{\Phi}]_{:,u}. \tag{26}$$

According to (26), the design of $\boldsymbol{Z}^{(u)}$ depends on $\boldsymbol{H}_e^{(u)}$. We adopt pilot-assisted channel estimation to estimate $\boldsymbol{H}_e^{(u)}$ as $\widetilde{\boldsymbol{H}}_e^{(u)}$ [12]. Based on the minimum mean squared error (MMSE) criterion, the designed digital precoder can be determined by

$$\widetilde{\boldsymbol{Z}}^{(u)} = (\widetilde{\boldsymbol{H}}_e^{(u)})^{\mathrm{H}}\left(\frac{P_T}{KU}\widetilde{\boldsymbol{H}}_e^{(u)}(\widetilde{\boldsymbol{H}}_e^{(u)})^{\mathrm{H}} + \sigma^2\boldsymbol{I}_K\right)^{-1}. \tag{27}$$

To satisfy the power constraint in (6), we need to normalize each column of $\widetilde{\boldsymbol{Z}}^{(u)}, u=1,2,\ldots,U$.

IV. Simulation Results

To evaluate the system performance, we set the number of the BS antennas as $N_{\mathrm{BS}}=128$. The number of OFDM subcarriers is set to $U=16$. We set the wideband mmWave channel parameters according to the delay model [3], including the maximum number of delay taps $D=4$, the sampling period $T_s = 1/1760$ μs and the roll-off coefficient $\beta=0.25$. The number of channel paths between the BS and the kth user for $k=1,2,\ldots,K$ is set to $L_k=4$, including a LoS path with the complex channel gain $\alpha_{1,k}\sim\mathcal{CN}(0,1)$ and three NLoS paths with the complex channel gain $\alpha_{l,k}\sim\mathcal{CN}(0,0.1), l=2,3,4$. We suppose the AoD of each path $\phi_{l,k}$ obeys the uniform distribution in $(-\pi/2,\pi/2]$ and the delay of each path $\tau_{l,k}$ obeys the uniform distribution in $[0,(D-1)T_s]$. We set the total transmit power $P_T=1$. The DLBA scheme is compared with the existing fully digital (FD) scheme, Hungarian scheme [8], TS scheme [7] and SOMP scheme [6].

As shown in Fig. 4, we compare the sum-rate performance for the five schemes at different SNR when $K=16$. We set $J=4$, which means each user has four candidate codewords to select. The performance of FD is provided as the upper bound. It is shown that the DLBA scheme achieves almost the same performance as the Hungarian scheme but outperforms the TS and SOMP schemes. When SNR = 20 dB, the DLBA scheme has 10.3% and 38.75% performance improvement over the TS and SOMP scheme, respectively, and has the almost the same performance as the Hungarian scheme. Note that both the TS scheme and SOMP scheme do not tackle the beam conflict, which substantially reduces the performance.

As shown in Fig. 5, we compare the averaged sum-rate for the five schemes with different K when SNR = 15dB. The averaged sum-rate is defined as the ratio of the sum-rate over K. It is shown that as K increases, the DLBA scheme drops more slowly than the TS and SOMP schemes, and has the same trend as the Hungarian scheme.

As shown in Fig. 6, we compare the running time for the five schemes with different K. To fairly compare the performance of different schemes, all schemes are implemented in Python 3.7 with TensorFlow-GPU 1.7.0 and executed on the same computer with a six-core processor, 16GB RAM and NVIDIA GeForce GTX 1660 Ti graphic card. The running time for different schemes grows, as K increases. It is seen that the FD scheme is the fastest, but it is only considered as the low bound and can not be implemented in practice. The DLBA scheme is faster than the TS, SOMP and Hungarian schemes, since it adopts the CNN to predict the beam allocation while the latter three schemes need iterative search to obtain the optimal solution.

V. Conclusions

In this paper, we have decoupled the analog precoder and the digital precoder by introducing the IF achievable rate. Then we have treated the beam allocation as a multi-label classification problem and have proposed the DLBA scheme. In order to avoid the beam conflict and maximize

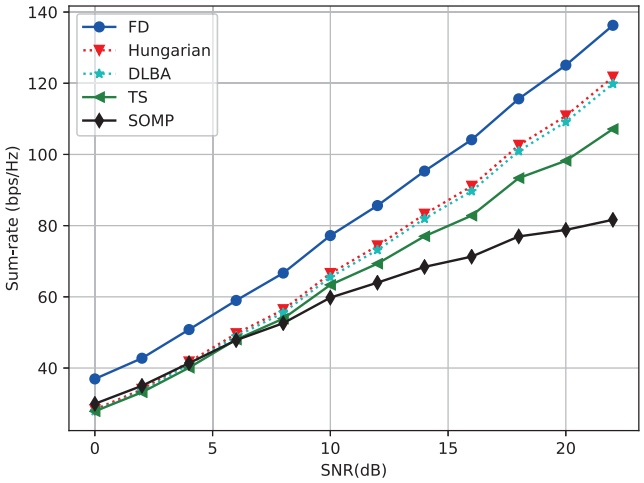

Fig. 4. Comparison of sum-rate performance for different schemes at different SNR.

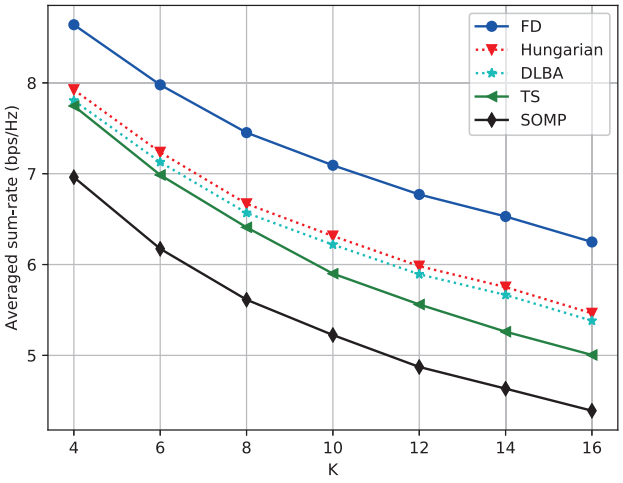

Fig. 5. Comparison of averaged sum-rate for different schemes and different K.

the sum-rate, we have proposed a conflict avoidance rule. Simulation results have demonstrated that the DLBA scheme can substantially reduce the computational complexity with a marginal sacrifice of sum-rate performance, compared to the existing schemes.

ACKNOWLEDGMENT

This work is supported in part by National Natural Science Foundation of China (NSFC) under Grant 62071116 and by National Key Research and Development Program of China under Grant 2021YFB2900404 and 2020YFB1807205.

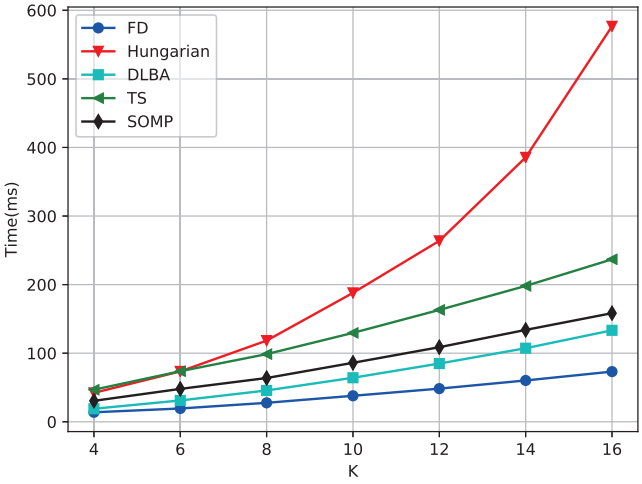

Fig. 6. Comparison of running time for different schemes in terms of K.

REFERENCES

[1] S. Han, C.-l. I, Z. Xu, and C. Rowell, "Large-scale antenna systems with hybrid analog and digital beamforming for millimeter wave 5G," *IEEE Commun. Mag.*, vol. 53, no. 1, pp. 186–194, Jan. 2015.

[2] C. Qi, P. Dong, W. Ma, H. Zhang, Z. Zhang, and G. Y. Li, "Acquisition of channel state information for mmWave massive MIMO: Traditional and machine learning-based approaches," *Sci.China Inf. Sci.*, vol. 64, no. 8, p. 181301, Aug. 2021.

[3] J. Rodríguez-Fernández, N. González-Prelcic, K. Venugopal, and R. W. Heath, "Frequency-domain compressive channel estimation for frequency-selective hybrid millimeter wave MIMO systems," *IEEE Trans. Wireless Commun.*, vol. 17, no. 5, pp. 2946–2960, May 2018.

[4] Z. Gao, C. Hu, L. Dai, and Z. Wang, "Channel estimation for millimeter-wave massive MIMO with hybrid precoding over frequency-selective fading channels," *IEEE Commun. Lett.*, vol. 20, no. 6, pp. 1259–1262, Apr. 2016.

[5] J. Bang, H. Chung, J. Hong, H. Seo, J. Choi, and S. Kim, "Millimeter-wave communications: Recent developments and challenges of hardware and beam management algorithms," *IEEE Commun. Mag.*, vol. 59, no. 8, pp. 86–92, Sep. 2021.

[6] O. E. Ayach, S. Rajagopal, S. Abu-Surra, Z. Pi, and R. W. Heath, "Spatially sparse precoding in millimeter wave MIMO systems," *IEEE Trans. Wireless Commun.*, vol. 13, no. 3, pp. 1499–1513, Jan. 2014.

[7] A. Alkhateeb, G. Leus, and R. W. Heath, "Limited feedback hybrid precoding for multi-user millimeter wave systems," *IEEE Trans. Wireless Commun.*, vol. 14, no. 11, pp. 6481–6494, July 2015.

[8] X. Sun and C. Qi, "Codeword selection and hybrid precoding for multiuser millimeter-wave massive MIMO systems," *IEEE Commun. Lett.*, vol. 23, no. 2, pp. 386–389, Dec. 2019.

[9] J. Suh, C. Kim, W. Sung, J. So, and S. W. Heo, "Construction of a generalized DFT codebook using channel-adaptive parameters," *IEEE Commun. Lett.*, vol. 21, no. 1, pp. 196–199, Sep. 2017.

[10] X. Sun, C. Qi, and G. Y. Li, "Beam training and allocation for multiuser millimeter wave massive MIMO systems," *IEEE Trans. Wireless Commun.*, vol. 18, no. 2, pp. 1041–1053, Feb. 2019.

[11] M. Lee, Y. Xiong, G. Yu, and G. Y. Li, "Deep neural networks for linear sum assignment problems," *IEEE Commun. Lett.*, vol. 7, no. 6, pp. 962–965, June 2018.

[12] W. Ma, C. Qi, Z. Zhang, and J. Cheng, "Sparse channel estimation and hybrid precoding using deep learning for millimeter wave massive MIMO," *IEEE Trans. Wireless Commun.*, vol. 68, no. 5, pp. 2838–2849, Feb. 2020.